Modeling the Lignin Degradation Kinetics in an Ethanol/Formic Acid Solvolysis Approach. Part 1. Kinetic Model Development

ARTICLE *in* INDUSTRIAL & ENGINEERING CHEMISTRY RESEARCH · JUNE 2012

Impact Factor: 2.59 · DOI: 10.1021/ie301487v

6 AUTHORS, INCLUDING:

James R. Gasson

12 PUBLICATIONS **94** CITATIONS

SEE PROFILE

Daniel Forchheim

Karlsruhe Institute of Technology

7 PUBLICATIONS **66** CITATIONS

SEE PROFILE

Ursel Hornung

Karlsruhe Institute of Technology

49 PUBLICATIONS **807** CITATIONS

SEE PROFILE

Andrea Kruse

Hohenheim University

124 PUBLICATIONS **3,918** CITATIONS

SEE PROFILE

I&EC research
Industrial & Engineering Chemistry Research

Article

pubs.acs.org/IECR

Modeling the Lignin Degradation Kinetics in an Ethanol/Formic Acid Solvolysis Approach. Part 1. Kinetic Model Development

James R. Gasson,[†,§] Daniel Forchheim,[‡,§] Tatjana Sutter,[‡] Ursel Hornung,[*,‡] Andrea Kruse,[‡] and Tanja Barth[†]

[†]Department of Chemistry, University of Bergen, Allégaten 41, NO-5007 Bergen, Norway

[‡]Institute of Catalysis Research and Technology, Karlsruhe Institute of Technology, Hermann-von-Helmholtz-Platz 1, DE-76344 Eggenstein-Leopoldshafen, Germany

Supporting Information

ABSTRACT: A formal kinetic model describing the main reaction pathways yielding demethoxylated monomeric phenols from wheat straw lignin in a hydrogen-enriched solvolysis reaction system using ethanol as cosolvent has been developed. The simplified lump model combines both a detailed focus on the deoxygenation reactions at molecular level as well as the reactions of global bulk lumps. The results show that depolymerization of lignin structures is quickly achieved and that deoxygenation reactions largely follow a main route pathway via intermediate methoxyphenols and catechols to give stable phenols in the liquid phase. Observed ethyl group substituents of phenolics are seen to originate from either alkylation reactions of the intermediates, or directly from the depolymerizing structures. A high correlation between primary 4-ethylphenol products and *para*-coumaryl units in the examined lignin suggests that main reaction pathways are strongly dependent on the type of plant lignin used.

INTRODUCTION

Complementing Lignocellulosic Bioethanol Production. Given today's global energy bottlenecks, the interest in sustainable production of biofuels and petroleum product replacements is more pressing than ever before. A strong research focus on lignocellulosic biomass exists, as it does not stand in competition with food and feed production. Hydrolytic separation of a substantial part of the hemicellulose and cellulose components from the whole biomass using acids or enzymes allows a high degree of depolymerization to sugars, followed by fermentation to deliver bioethanol in high yields. The third component (comprising roughly $^1/_3$ of lignocellulose materials) is lignin, which is mostly seen as waste. The major amount is used for cofiring purposes to produce energy within the ethanol production plants. From a chemical perspective, it is a readily available source of aromatics and phenolics that are present within the structure. These compounds are of great interest for use as platform chemicals, and produced bio-oils could possibly also be used as an unresolved mixture for fuel blending purposes after refining. Producing e.g. selected hindered phenols, which are currently added to turbine fuels because of their antioxidative properties,[1] is just one way of making better use of this potential resource. A first prerequisite for such exploitation is, however, the development of an economical depolymerization and deoxygenation process of the lignin structures to its monomeric units.

The Lignin-to-Liquid Approach. Lignin depolymerization and valorization by hydrodeoxygenation has been widely explored within different pyrolysis and solvolysis approaches. Solvolysis provides the advantages of mild conditions and a single-phase evironment due to the miscibility of the organic products in the (supercritical) solvent. Ethanol has a very high solvency for biomass and a low critical temperature which makes it attractive for lignin depolymerization.[2] Further advantages of solvolysis in ethanol over fast pyrolysis are a less oxygenated oil fraction[3] and almost no solid residue (<5%).[4,5] The Lignin-to-Liquid (LtL) concept uses high temperature (623−663 K) and high pressure (20−30 MPa) conditions over a time interval of 4−16 h in an ethanol solvent medium. In situ hydrogen donation is achieved by the thermal degradation of formic acid. In comparison to commonly used hydrogen gas in other hydrogenation approaches, e.g., by Forchheim et al.,[6] formic acid degrades to a very active atomic hydrogen species,[4] resulting in successful deoxygenation and hydrogenation of lignin structures to yield various largely demethoxylated phenolics comprising a high H/C and low O/C ratio bio-oil,[3] without necessitating any further added catalyst for activation or transfer.

Lignin: A Variable Polymer. Common challenges in the degradation of lignin to bio-oils rich in selective phenols include the degree of depolymerization, deoxygenation and hindrance of repolymerization reactions. In contrast to sugar polymers, the structural and chemical variations encountered in lignins from different origins further encumber the understanding of degradation mechanisms and complicate the tailoring of a refined product. Varying amounts of the three characteristic phenylpropane building blocks, shown in Figure 1, are found depending on the type of lignin.[7]

Softwoods are commonly composed of guaiacyl lignin, which is principally made up of coniferyl moieties. Guaiacyl−syringyl lignin contains a combination of sinapyl and coniferyl moieties which are prevalent in hardwoods. Annual plant or grass lignin is mainly composed of *para*-coumaryl units.[8] The characteristic

Received: March 12, 2012
Accepted: June 26, 2012
Published: June 26, 2012

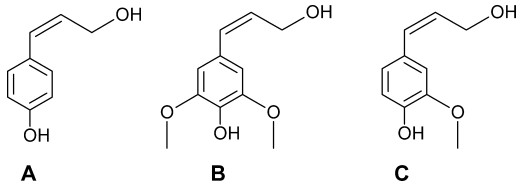

Figure 1. Three characteristic monolignols which constitute the characteristic monomeric units of lignin: A: *para*-coumaryl alcohol; B: sinapyl alcohol; and C: coniferyl alcohol.

variation of these different units can also be observed in the depolymerized products.[9] Within this work, wheat straw lignin is used, thus monoaromatic products will largely be derived from abundant *para*-coumaryl alcohol units.

Further factors influencing the wide palette of products depend on the separation method of the lignin from whole biomass and the thermochemical conditions chosen to degrade the lignin, especially the temperature, and the type of reactor.

Lignin Degradation. In the LtL approach, a time-dependent transition from methoxylated phenolic structures to C_1-C_4 hydrocarbon-substituted demethoxylated phenols is observed. Although the experiment is conducted as a single-step reaction, it is unclear if depolymerization and deoxygenation reactions take place consecutively (guaiacol → catechol → phenol), as observed under pyrolysis conditions,[10] or if other competing degradation pathways, e.g. omitting catechol as an intermediate, are prevalent.[9] Furthermore, it is not clear at which stage in this process alkylation of the phenolic rings, presumably by the solvent ethanol, takes place. LtL conditions differ largely from other systems which have been previously investigated, and the combination of ethanol and homogeneous in situ hydrogen donation might therefore suggest alternative pathways. From an economic point of view, it is vital to confirm reaction pathways and identify bottleneck steps in a kinetic analysis to work toward more economic reaction conditions and catalyst implementation.

Experimental studies of the feedstock decomposition and charting of reaction pathways under pyrolysis conditions have been widely investigated. The studies were conducted with or without the presence of hydrogen in combination with a heterogeneous catalyst, and are largely based on available intermediate model substances as starting materials, such as syringol, guaiacol, and catechol, to try and master the cascade of demethoxylation, deoxygenation, hydrogenation, alkylation, demethylation, and methanolization reactions within such processes.[11−13] Similar experiments have also been performed for lignin.[10,11,14] Experiments carried out with protic alcoholic solvents on both lignins and lignin model compounds have shown an increased dispersion/solution of lignin, thus giving low average yields of insolubles after pyrolysis.[3,15] Furthermore, ethanol is seen to be incorporated into the phenolic structures through alkylation reactions.[16,17] Hydrogen donors can further inhibit repolymerization reactions of monomeric and oligomeric structures by capping free radicals and thus increasing the yield of the monomers.[9,15]

Kinetic models describing the decomposition of lignin are limited and are largely concentrated on global bulk models describing the yields of gas, char, and liquids. First attempts describing the degradation on this level were done using a single first-order reaction,[18] which were followed by more complex models, involving also multiple competing reactions.[19] Different modeling approaches for both lignin and biomass degradation have been comprehensively summarized by Miller and Bellan, Prakash and Karunanithi, and Brebu and Vasile.[20−22] Reaction kinetic studies under hydrothermal conditions have been performed both based on lignin[23] and guaiacol.[24] To the best of the authors' knowledge, however, no model has so far been reported that is able to describe not only the formation of bulk materials, such as gas and char, but also the formation and hydrodeoxygenation of phenolic components from lignin degradation.

This Work. One of the principle ideas behind the LtL approach is to retain the valuable chemical structures in the lignin, by depolymerizing and deoxygenating them to give demethoxylated monoaromatic units, and thereby enhancing quality and value of the produced bio-oil. The critical reaction steps are part of a larger reaction network, comprising various reaction pathways from lignin not only to bulk products, but also to the desired demethoxylated phenolics. The reactive solvent ethanol further increases the complexity of the reaction scheme. The influence of ethanol, in situ hydrogen donor, and reaction time on both intermediate and target species in the LtL approach are here to be further explored by developing a formal kinetic model, comprising both molecular level phenolic reactions and global bulks.

For validation of the formal kinetic model, the mathematically optimized formal rate coefficients of the defined reaction pathways and the fits of calculated and experimental values are discussed.

MATERIALS AND METHODS

Materials and Reactors. Formic acid, absolute ethanol, and analytical consumables were acquired from Sigma Aldrich, Germany in highest available quality and were used without any further purification. Protobind 1000, a lignin-rich (>90 wt %) material produced from wheat straw, was received from ALM India Pvt. Ltd., India. This was dried for 48 h at 353 K and ground to a maximum diameter of 200 μm. Elemental analysis showed C (63.8 wt %), H (6.0 wt %), and O (27.0 wt %), resulting in a H/C atomic ratio of 1.1 and an O/C atomic ratio of 0.3. Residual moisture of the biomass residue after drying and storage was measured to be 4.5 wt %.

Custom-built, 5-mL batch reactors made of 1.4571 stainless steel were used for all experiments. These have an inner cylindrical shape with a diameter of 11.5 mm and 48.1 mm height. The reactors have a metal on metal seal and can withstand pressures of up to 40 MPa and a maximum temperature of 673 K. The reactors were heated in a HP-5890 GC oven, which can be heated and cooled using a temperature program.

Experimental Section. Ten experiments were conducted using a mixture of 0.33 g of lignin, 0.27 g of formic acid, and 2.0 g of ethanol. The loadings were chosen to enable a good analysis of the system and to minimize the influence of absorption processes on char particles by selecting a low level input of lignin in high dilution. The reactions were carried out at a constant 633 K and reaction durations of 15, 30, 45, 60, 90, 120, 240, 360, 480, and 1180 min. Replicate experiments were performed for 60, 120, and 240 min reaction durations to assess experimental uncertainty.

The reactors were filled with a solution of ethanol, formic acid, and biomass, then purged with nitrogen and sealed. They were then heated with a heating rate of 40 K/min. Reaction time is defined to start when the set temperature of 633 K is reached. After completion of the reaction duration, the reactors were removed from the oven and rapidly quenched in icy water.

The reactors were then ventilated, and the gas was quantified volumetrically and sampled on GC. The liquids and solids were recovered thereafter, the latter being weighed, dried for 16 h at 378 K, and reweighed to account for liquid loss. The solids were analyzed on FT-IR. The filtered and quantified liquids were routinely sampled on GC-FID and on GC-MS. Water content analysis for selected samples was performed by Karl Fischer titration.

Analytical Procedures. *GC Analysis of the Gases.* Gas-phase GC analysis was performed on an Agilent 7890A with a 2-m Molsieve 5A column in series with a 2 m Porapak Q column equipped with a FID front and TCD back detector. The system was controlled by an Agilent laboratory data system. Injections were carried out by manually injecting 100 μL of the ventilated gas from the reactor. Temperature program was as follows: initial temperature 323 K for 22 min, then heating at 20 K/min to 423 K, kept for 15 min; further heating at 50 K/min to 503 K, kept for 10 min. The injection port was at 523 K, the FID was at 503 K, and the pressure was kept constant at 255 kPa. Components were quantified by varying amounts of standard gas mixtures.

GC-FID Analysis of the Liquids. Quantitative GC-FID analysis of liquid products was performed on a HP 5890-II GC equipped with HP autosampler 5890, a 30-m Rtx-1MS dimethyl-polysiloxan column, and FID detector. The system was controlled by an HPChem laboratory data system. Temperature program was as follows: initial temperature 313 K for 6 min, then 5 K/min heating to 453 K, then with a rate of 30 K/min continued heating to 533 K, kept for 5 min; further heating increase at 30 K/min to a final 573 K and kept for 12 min. The injection port had a temperature of 548 K and the FID was at 603 K. The crude liquid samples were diluted in a 1:2 ratio with a prepared standard solution of pentacosane in ethyl acetate (1002 mg/L) as an external standard and injected by the autosampler system. Monoaromatic components were individually calibrated for quantification by running dilution series in a manner identical to that of the samples.

GC-MS Analysis of the Liquids. Qualitative GC-MS analysis of liquid products was carried out on a Trace Ultra GC coupled with a DSQ II quadrupole MS detector from Thermo Scientific. The samples were diluted in a 1:100 ratio in dichloromethane and were analyzed using split injection at 523 K (injector temperature) on a 25-m ULTRA 2 silica column ((5% phenyl)-methylpolysiloxane) from Agilent Technologies. A constant gas flow rate of 1 mL/min and a split ratio of 100 with the following temperature program were applied: initial temperature 313 K, increased at 6 K/min to 473 K, further increased with 8 K/min to a final 573 K, kept for 5 min. The MS detector was operated in positive ionization mode at 70 eV with an ion source temperature of 473 K.

Karl Fischer Titration. Karl Fischer titration was used for the determination of the amount of water in selected samples. Samples were evaporated in a Metrohm 774 oven processor at 651 K. Carbonic acid was extracted from the evaporated gas and led into the titration cell. A volumetric method titration was performed with titrant solution Hydranal Composit 5. The end point of the titration was marked with the bipotentionmetric method.

FT-IR Spectroscopy. FT-IR analysis of the feed material and collected solid residues was performed by preparing and pressing conventional KBr analyte pellets and analyzing these on an FT-IR Varian 660-IR in linear transmittance mode. Thirty scans were performed after background subtraction and the results were averaged. The measurement data were later normalized to compensate for concentration effects.

Delplot Analysis. The Delplot technique is based on the analysis of selectivity-conversion plots and can be used for both primary and higher rank products.[25] The basic primary Delplot allows the separation of primary from nonprimary reactions for any given reaction order. For a primary Delplot, the yield of a singular ith component (y_i) divided by the overall conversion (x) is plotted over x. Plotting y_i/x^2 over x gives a second rank Delplot, y_i/x^3 over x gives third rank, and so on. The intercept on the y-axis stipulates the rank of the product. If the intercept in a primary rank Delplot of a component is finite, the product is a primary one. If the intercept on the y-axis is zero, then the component is not formed by a primary reaction. The interpretation of intercepts is analogous for higher ranks.

Modeling. Modeling was performed in Matlab V 7.12.0, MathWorks using a set of differential equations, which were formulated according to the reaction scheme elaborated with the techniques described above. Both the differential equations and chemical reactions on which these are based are included in the Supporting Information. The scheme is comprised of a number of l defined (lump) components and n reaction pathways. For each reaction pathway a rate coefficient is defined. The reaction order for all reactions is set to one.

The unconstrained nonlinear optimization Matlab-function "fminsearch", which uses the simplex search method by Lagarias et al.,[26] was used for optimization, because of its robustness and because it does not need derivatives of the objection function. The function "fminsearch" finds the minimum of the scalar function given in eq 1, starting at $k_{i=1,2,...,n} = 0.01$:

$$f(k_1, k_2, ..., k_n) = \sum_i \sum_j \exp\left(w_{i,j}\left[y_{i,j}^{meas} - y_{i,j}^{calc}(k_1, k_2, ..., k_n)\right]\right) \quad (1)$$

where

$$y_{i,j} = \frac{m_{i,j}}{m_{L,0}} \quad (2)$$

and

i = index of products
j = index of experiments
$m_{i,j}$ = normed masses of species i in experiment j
$m_{L,0}$ = input mass of lignin
$w_{i,j}$ = weight factor of species i in experiment j
k = reaction rate coefficient of the total number of n reactions.

The values for $y_{i,j}^{calc}$ were determined using a set of differential equations expressing the overall kinetics of the developed model. It should be pointed out that a chemical reaction model would only then be able to describe the experimental data correctly if all the relevant reaction pathways were contained in the model. The ultimate number of reactions (and rate coefficients k) in a model is of minor significance.

RESULTS

Product Analysis and Quantification. *General.* The products of the LtL approach comprise three major phases in varying ratios: gas, solid, and liquid phase. The recovered amounts of these three phases are dependent on reaction time, and are illustrated in a global mass balance diagram in Figure 2. The decomposition of formic acid at 633 K contributes largely to the initial high gas yields. Extended reaction time shows a

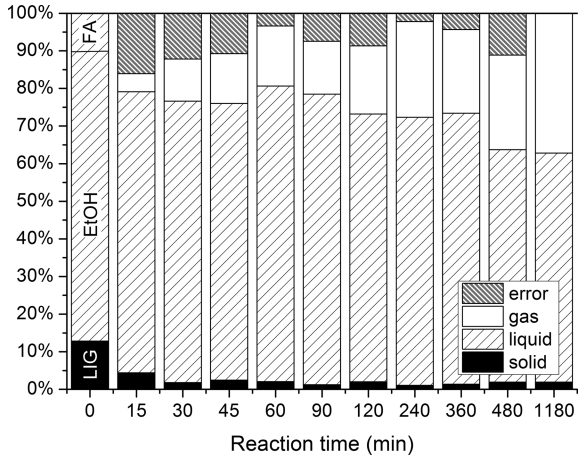

Figure 2. Liquid, gas, and solid reaction products at varying reaction durations compared with the input amounts of lignin (LIG), ethanol (EtOH), and formic acid (FA) at reaction time zero of the experimental series. All experiments were conducted at the same loading conditions: 0.33 g of lignin, 0.27 g of formic acid, and 2.0 g of ethanol and a reaction temperature of 633 K.

continued growth in the amount of gas and a reduction of the single liquid phase obtained. Minimum amounts of solid residue in reference to the amount of input lignin are reached at 90 min (1.2 wt %) and 240 min (1.0 wt %). Although pressures in the reactors could not be measured, comparable experiments in a larger batch reactor have shown reaction pressures between 29 and 33 MPa.[27] Based on the decreased formic acid to ethanol loading ratio, the pressure in the presented experiments is expected to be reduced by 3−6 MPa.

Gas Phase. Analyses of the different components comprising the gaseous phase, Figure 3, show that up to 1.9 wt % of CO

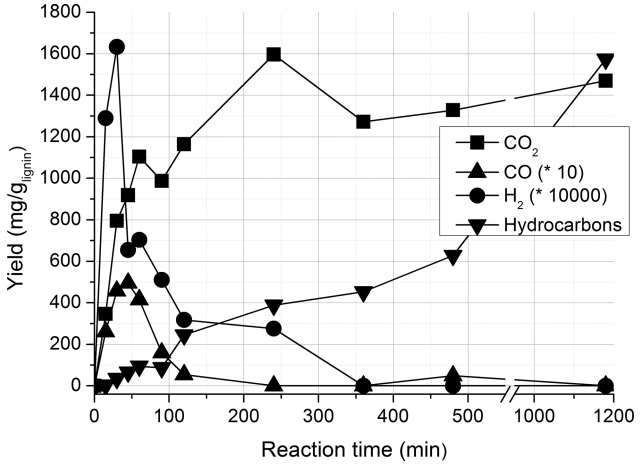

Figure 3. Individual yield of the gaseous product components, quantified on GC-FID and GC-TCD. The values for CO and H_2 have been multiplied by factors of 10 and 10 000, respectively, to enable better visibility on the given scale.

is produced at low reaction times. The yield, however, quickly decreases to be replaced by a rapid increase of CO_2. Although H_2 is detected, it is only present in minor amounts of some 0.01 wt % and further diminishes with increased reaction time. Degradation of formic acid has been reported to occur via two different pathways, yielding either CO and H_2O or CO_2 and H_2.[28] The alcoholic cosolvent has been seen to influence the ratio of the two main degradation pathways of formic acid to yield CO_2 and H_2 or CO and H_2O in a roughly 3:2 ratio.[29] The rapid consumption of H_2 suggests a central function and fast incorporation in the depolymerization of the polymeric lignin structures. The continued increase in total amount of gaseous products and the formation of hydrocarbon gases (including CH_4, C_2H_6, C_2H_4, C_3H_8, C_3H_6, C_4H_{10}) points toward the importance of gasification and cracking in later phases of the reaction process.

Solid Residue. To determine the degradation rate of the present lignin structures, the solid residue in the reactors was weighed after the reaction was terminated. However, due to repolymerization reactions causing an increase of solids after an initial decrease, additional analyses of the solids were required to allocate the transition point between a predominantly unreacted lignin-type structure and polyaromatic char, see Figure 4.

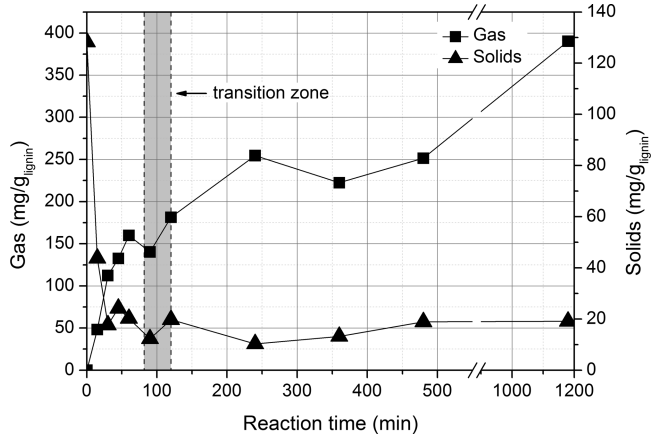

Figure 4. Gas and solid residue yields for experiments carried out at varying reaction times. A transition zone, indicating the change from largely lignin characterisic solids to char is indicated, utilizing the results from FT-IR analysis.

To estimate the degree of depolymerization and conversion of lignin, as well as the transition to coking, FT-IR spectra of the solid residues and a sample of the input biomass were taken. Figure 5

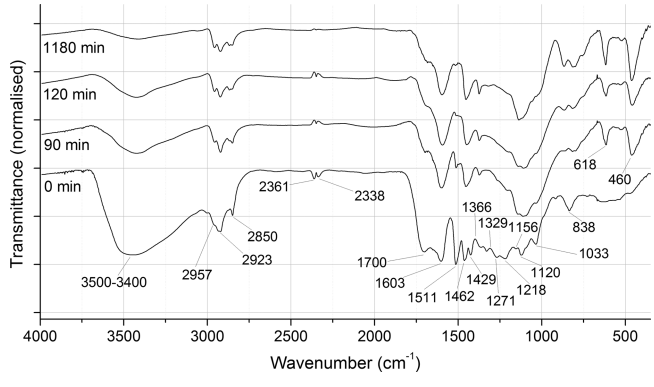

Figure 5. FT-IR spectra of unreacted lignin and of the collected solid residues at 90, 120, and 1180 min reaction duration. The largest alterations take place during the first 120 min and are documented in Table 1.

shows the FT-IR spectrum of the unreacted lignin with labeled characteristic absorption bands. The spectrum reflects the predominant aromatic ring structures with hydroxyl and C−O moieties. The relatively identical intensities of the absorption

dx.doi.org/10.1021/ie301487v | *Ind. Eng. Chem. Res.* 2012, 51, 10595−10606

bands at 1511 and 1603 cm^{-1} indicate an increased ratio of syringyl relative to gauaiacyl moieties in the polymer.[30] The largely abundant *para*-coumaryl moieties do not enable a characteristic band allocation. All allocated origins of bands and their alterations throughout reaction time are summarized in Table 1.

Large alterations can be observed in the FT-IR spectrum of the solid residues within the first 120 min reaction duration; see Figure 5 for four example spectra taken from the lignin and solid residues from the reactors after 90, 120, and 1180 min. The most dominant alteration is the disappearance of hydroxyl functions, which is seen in the decrease of the broad −OH stretching band at 3500−3400 cm^{-1}. Decreasing absorbance of aromatic ring vibrational bands (1603, 1511, 1429, 1366 cm^{-1}), especially in combination with C═O stretching (1700, 1329, 1271, 1218, 1033 cm^{-1}) are clearly visible, illustrating the decomposition to monoaromatic units, and their solubilization in the oil. These bands play a role in estimating the transition period from a largely lignin-like structure to a polyaromatic char. Roy et al. quantified the content of lignin, using the aromatic ring vibrational band at 1511 cm^{-1}.[31] Analysis of our collected FT-IR data shows the disappearance of this band between 90 and 120 min with the largest decrease occurring in the first 45 min, as illustrated in Figure 6.

Liquid Analysis. The liquid single-phase recovered was of a dark brownish color and had a pungent odor. The single phase remained stable, without any precipitation, phase separation, or change of chemical composition as observed by GC analysis, also after several weeks of storage at 278 K. For analysis, the crude product was evaluated without further separation, thus retaining the original amount of remaining ethanol and process water. The water content was found to increase from 3.9 wt % at 30 min to 14.7 wt % at 1180 min reaction time.

The chromatogram in Figure 7 shows a typical product spectrum for intermediate reaction times, where demethoxylated phenols, methoxylated aromatics, and hydroxy- and dihydroxybenzenes are the dominant components. Typical substitutions include 4-methyl and 4-ethyl substitutions. Increased reaction durations yielded more complex chromatograms with numerous additional peaks, which were identified by GC-MS to be various hydrocarbon substituted demethoxylated phenols.

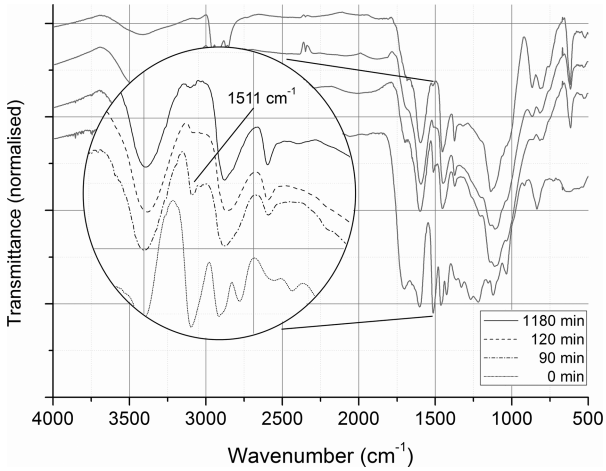

Figure 6. Zoom of the FT-IR region around the functional aromatic ring vibration band at 1511 cm^{-1}, which is used for identification of the transition period from largely lignin dominant structures to polyaromatic char of the solid residue.

One major focus of the kinetic model is the selected key components, which represent the different compound classes. These quantified compounds are listed in Table 2 and are also illustrated in Figure 7. For the monoaromatic compounds quantified in the liquid phase, the following averaged maximum errors for the single replicates were found (standard deviation given in brackets): methoxyphenols = 0.88 mg/g_{lignin} (5.3%), catechols = 0.36 mg/g_{lignin} (2.3%), phenols = 0.1 mg/g_{lignin} (1.0%), and 4-ethylphenol = 0.38 mg/g_{lignin} (2.9%). The errors are considered to be within an acceptable range; furthermore,

Table 1. Characteristic FT-IR Absorptions and Observed Changes between the Biomass Feed and the Solid Residue Samples

observed band (cm^{-1})	literature (cm^{-1})	origin[15,32−34]	peak characteristics in unreacted lignin	peak alterations in solid residue
3500−3400	3450−3400	−OH stretching	broad	initial strong decrease
2957, 2923, 2850	2940−2820	−OH stretching in methyl and methylene groups	very weak, intense, weak	strong decrease at 2923 cm^{-1}
2361 and 2338			weak	constant decrease
1700	1715−1710	C═O stretching nonconjugated to the aromatic ring		disappears after 30 min
	1675−1660	C═O stretching in conjugated to the aromatic ring		
1603	1605−1600	aromatic ring vibrations	intense	decreases
1511	1515−1505	aromatic ring vibrations	intense	disappears after 120 min
1462	1470−1462	C−H deformations (asymmetric)		
1429	1430−1425	aromatic ring vibrations		disappears after 30 min
1366	1370−1365	C−H deformations (symmetric)	weak	intensifies
1329	1330−1325	syringyl ring breathing with C−O stretching	weak	disappears after 45 min
1271	1270−1275	guaiacyl ring breathing with C−O stretching		disappears after 45 min
1218	1220	syringyl ring breathing	weak	disappears after 60 min
1156	1160	aromatic C−H in plane deformation, guaiacyl type	weak	
1120	1120	aromatic C−H in plane deformation, syringyl type	weak	
1033	1030	aromatic C−H in plane deformation guaiacyl type		
		and C−O deformation of primary alcohol		disappears after 45 min
917			weak	
867				appears at 240 min
838	834	*para*-substituted aromatic group		disappears at 90 min
810				appears at 240 min
618				appears at 90 min
460				appears at 90 min

dx.doi.org/10.1021/ie301487v | *Ind. Eng. Chem. Res.* 2012, 51, 10595−10606

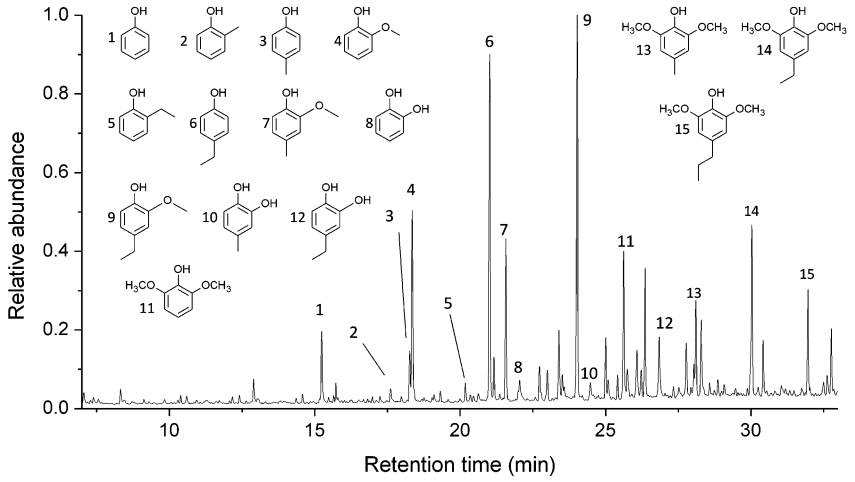

Figure 7. Chromatogram of a product oil produced at 633 K and 90 min reaction time. Dominating phenolic species are found as main peaks in the chromatogram. Quantified key compounds are listed in Table 2.

Table 2. Monoaromatic Products Quantified by GC-FID

compound class	no.	name	molecular formular	retention time (min)
methoxyphenols	4	guaiacol	$C_7H_8O_2$	18.36
	7	4-methylguaiacol	$C_8H_{10}O_2$	21.58
	9	4-ethylguaiacol	$C_9H_{12}O_2$	24.03
	11	syringol	$C_8H_{10}O_3$	25.63
catechols	8	catechol	$C_6H_6O_2$	22.05
	10	4-methylcatechol	$C_7H_8O_2$	24.48
	12	4-ethylcatechol	$C_8H_{10}O_2$	26.85
phenols	1	phenol	C_6H_6O	15.25
	2	2-methylphenol	C_7H_8O	17.61
	3	4-methylphenol	C_7H_8O	18.27
	5	2-ethylphenol	$C_8H_{10}O$	20.18
	6	4-ethylphenol	$C_8H_{10}O$	21.02

consistent trends for the development over reaction time of all phenolic products are clearly visible in Figure 8.

The focus of the liquid analysis is to evaluate the monomeric phenolics in terms of their yields as a function of reaction time. For this, different phenolics were grouped according to their degree and type of oxygenation. Their time-dependent yields are given in Figure 8. 4-Ethyl substitution is the dominant substitution for all species. In addition, 2-ethyl and 2- and 4-methyl substituted phenolics were quantified and included in some of the compound classes.

Figure 8a shows the methoxylated phenolics, which show an initial rapid increase and following decrease after circa. 90 min. The, by comparison, more rapid decrease of syringol supports the previously observed conversion of syringol to guaiacol.[9] In general, all methoxylated phenolics, including syringol, show a large similarity in their time-dependent yield profile. A B-spline function based on averaged values of the single constituents helps to illustrate the overall trends. The profile suggests the single constituents to be primary products within our analysis focus, and subsequently the rapid decrease in concentration supports their identification as intermediates.

According to several investigations conducted under pyrolysis and hydrolysis conditions,[10,35] catechols are found to be products of the secondary decomposition of methoxylated phenolics.

Figure 8b shows the different quantified catechols as well as the averaged trend function. A somewhat slower initial increase in comparison to the methoxylated species with lower yields is found, together with a slight decrease at over 90 min reaction time. However, the two values for catechol at 240 and 1180 min differ largely from the values for the substituted species, breaking with the generally decreasing yields. These high values were treated as outliers for further analyses.

The dominance of 4-ethyl substituted species is especially noticeable for 4-ethylphenol in Figure 8c. Indeed, the rapid yield increase of this compound can be compared more to the increase of the methoxylated phenolics than to other constituents of the phenol parent structure. The slow decrease over time however suggests that it is a more stable product within the degradation and reaction pathways of the monomeric units. The other nonmethoxylated phenolics show a very slow yield increase, which, when averaged, remains at a roughly constant yield value after 240 min reaction time. The initial strong increase of 4-ethylphenol suggests a different reaction pathway compared to the rest of the phenols.

Demethanization and deoxygenation reactions link the different compound classes, however the overall yield shows that a large proportion of the components is lost when increasing the reaction time. This is due to char-formation or gasification processes.

Kinetic Model Development. *Discerning the Rank of Key Reaction Steps.* Delplot analysis was performed to confirm the indicative ranks of the phenolic species as seen in the time-dependent yield plots in Figure 8.

Singular components were lumped according to their compound classes and time-dependent yields, see Table 2 for reference. The one exception being 4-ethylphenol, which showed a considerably different yield characteristic over time from the rest of the phenols and was thus considered individually. Due to the uncertainty of the compositional transition from lignin to char, the necessary overall conversion rate for Delplot analysis was approximated by summing up all quantified monoaromatic species in the liquid. Full conversion is described by a maximum yield (indifferent as to the different classes involved) for all of these components. This is reached at 60 min reaction time, after which the total yield declines, first slightly and then more rapidly.

Figure 9 shows the first rank Delplot with the 3 component lumps and 4-ethylphenol. The intercepts of the extrapolated trend lines toward zero conversion show that the methoxylated

dx.doi.org/10.1021/ie301487v | Ind. Eng. Chem. Res. 2012, 51, 10595−10606

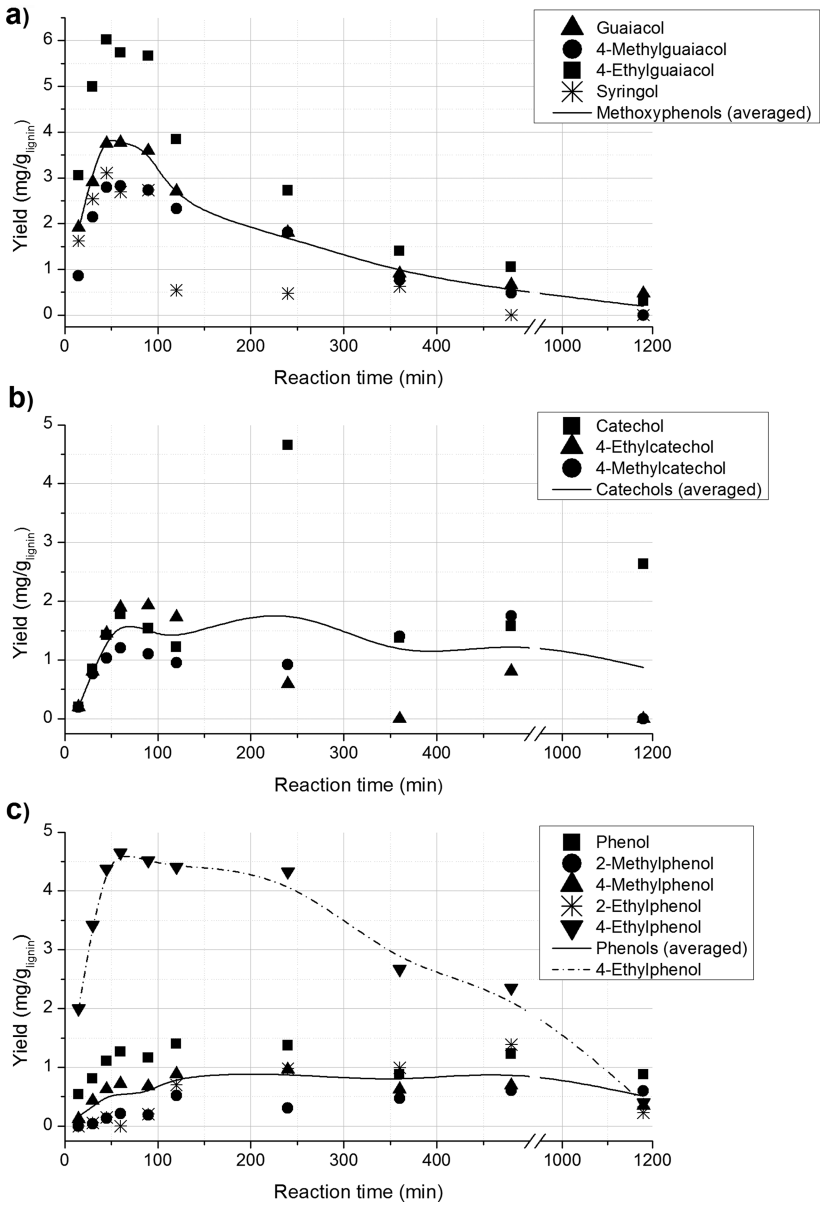

Figure 8. Yields of key components for the different phenolic compound classes: (a) methoxyphenols, (b) catechols, and (c) phenols over reaction time.

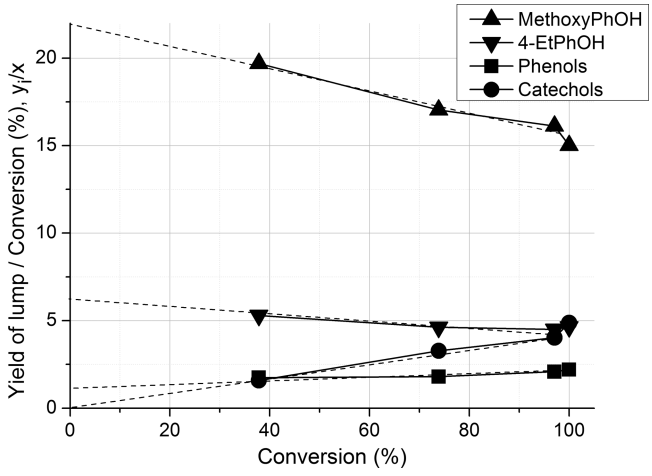

Figure 9. First rank Delplot for monophenolics showing a finite *y*-axis intercept for methoxyphenols, phenols, and 4-ethylphenol. A zero intercept is found for catechols.

phenols and 4-ethylphenol are clearly finite, indicating them to be primary products. Clearly, considering the possible decomposition of syringol to form guaiacol, the latter can also be a secondary product. However, this reaction pathway was not considered in this work. The extrapolated intercept of the *y*-axis, at the value zero, for the catechol lump shows it to be of a higher rank and thus at least a secondary product. The phenol lump intercepts the *y*-axis slightly under the value of 1. This suggests phenols to be a primary product within the reaction network. Multiple reaction pathways yielding the various products can of course occur in such a complex system, also with varying ranks, requiring further exploration.[36] However, due to the complexity of our model and multitude of unknowns within the reaction pathways, use of the interpretation extensions could not be applied. Competing and parallel reactions must be expected, but the analysis performed here is restricted to identification and description of the major pathways at given reaction conditions, while still recognizing that further reactions exist. Reviewing the plots of the primary product 4-ethylphenol suggests multiple pathways of quantitative

dx.doi.org/10.1021/ie301487v | *Ind. Eng. Chem. Res.* 2012, 51, 10595−10606

significance that could potentially also produce other phenols directly from the biomass as primary products. The interpretation for this component is tentative, as the extrapolation based upon four data points introduces a large degree of uncertainty in the determination of the *y*-axis intercept.

The second rank Delplot in Figure 10 shows that all *y*-axis are now finite, thus categorizing catechols as secondary products. The other intercepts diverge.

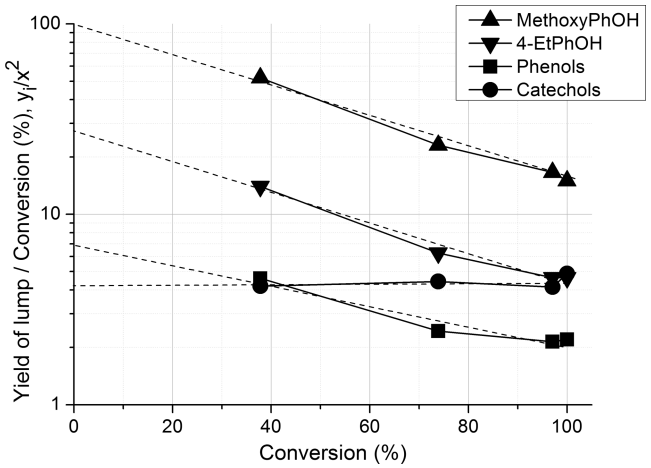

Figure 10. Second rank Delplot for monophenolic compounds indicates catechols to be of higher rank order.

The evaluations for guaiacols and catechols coincide with the findings by Jegers and Klein under pyrolytic conditions.[10]

Formulating a Model Pathway. In terms of the wide product spectra observed in these reactions, a lump-model is expected to be the best approach and the analysis is focused on identifying and describing the significant reaction pathways. Single components which have been quantified in the course of the experimental work were used in the modeling, as well as global bulk components. This allows the mapping of the complete pathway from the biomass to specific target compounds, such as phenol. Observations made in the experimental part of this study, as well as literature knowledge, are combined to formulate the model presented in Figure 11.

Under given temperature conditions, lignin is seen to depolymerize efficiently and quickly. Solid residue detected after more than 2 h reaction is assumed to mainly originate from repolymerization reactions of phenolic compounds, such as catechols or phenols.[37] The solid residue values were thus defined as unreacted lignin (<2 h) or char (>2 h).

Guaiacol has been stipulated as one of the key intermediates that forms phenols and catechols from lignin. The main reactions of the characteristic substituents of this compound class within our analysis are the demethanization to give catechol (k_2), the hydrolysis in the presence of H_2O to yield methanol and catechol,[35] and the loss of CO to yield phenol. The production of gas from these reactions however cannot be used for evaluation, as the volumes are far smaller relative to the gas formed from formic acid and ethanol (k_{12}, k_{13}). The catechols produced are in addition also reactive species, seen to decompose further to phenols (k_4).[10]

This general sketched pathway is further accompanied by de- and alkylation reactions by the reactive alcohols present (k_7–k_9, k_{14}).[17] Alkylation reactions are very dependent on the substituents attached to the aromatic ring, and prior studies suggest that alkylation reactions would be largely preferred by guaiacols.[16] The abundance of 4-methyl and -ethyl substituents observed for guaiacols, which are also present in catechols and phenols, suggests the alkylation to take place either immediately from reactive species during the depolymerization process, or as a very fast reaction from guaiacol, rendering 4-ethylphenol to be the most abundant of this compound class. Either way, the initial reaction time step chosen is not able to describe this reaction, and as the alkylation pattern of the *para*- position is subsequently seen in both catechols and phenols, lumping of the different alkylations is used. 2-Ethyl substitution is however, in significant quantities, only found for phenols. Thus, a separate *ortho*-alkylation is proposed for 2-ethylphenol (k_8), to explore the importance of this reaction.

All gaseous and inorganic liquid products, namely CO_2, CO, H_2, H_2O, and hydrocarbon gases (HC-gases), such as CH_4, C_2H_4, C_2H_6, C_3H_6, C_3H_8, C_4H_{10}, were summed under the model lump component "gas". Furthermore, L_D (depolymerized lignin) is a lump component containing all components derived from lignin that are not detected or quantified by GC, but however,

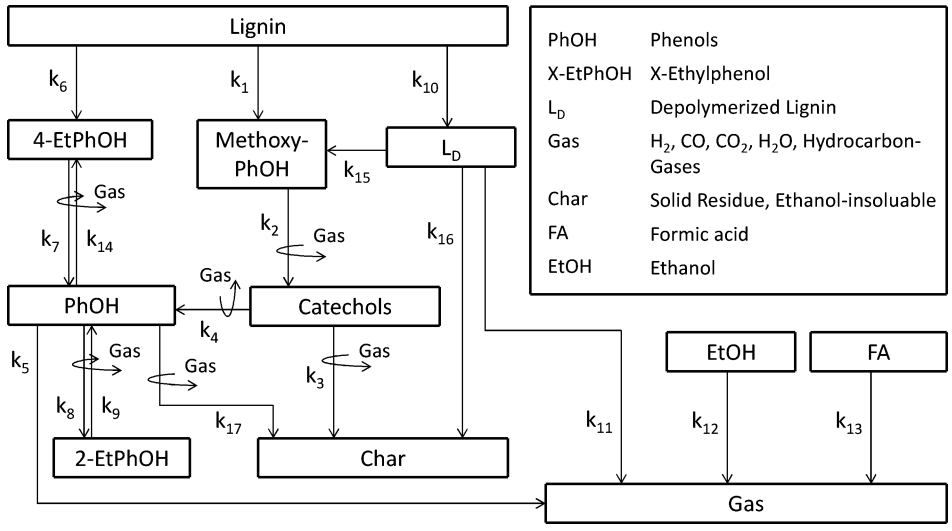

Figure 11. Scheme of main reaction participants and pathways of the depolymerization of wheat straw lignin; gaseous products of ethanol and formic acid gasification take part in reactions 2–4, 7–9, 14, and 17. This is indicated by curved arrows.

dx.doi.org/10.1021/ie301487v | *Ind. Eng. Chem. Res.* 2012, 51, 10595–10606

are soluble in ethanol, i.e. can not be categorized as solid residue or gas.

Kinetic Study Results. Different variations of the model shown in Figure 11 were considered, including additional reaction pathways, among them the direct conversion from guaiacol to phenol. After evaluating the results of the minimum search, the model version presented in Figure 11 was concluded to be the most appropriate. The focus was put on a good mathematical fit for phenolic products, see Figure 12. The model

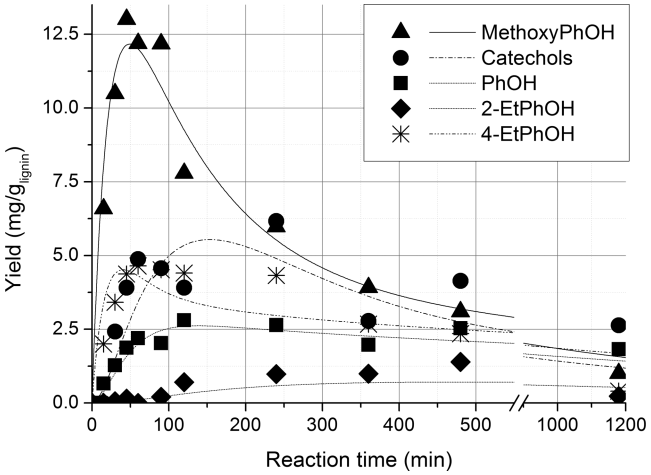

Figure 12. Experimental values compared with the model fit functions for the quantified key phenolic compounds.

also allowed a good fit of the bulk gaseous products and solid residue amounts, see Figure 13. Comparing the 3 rate coefficients

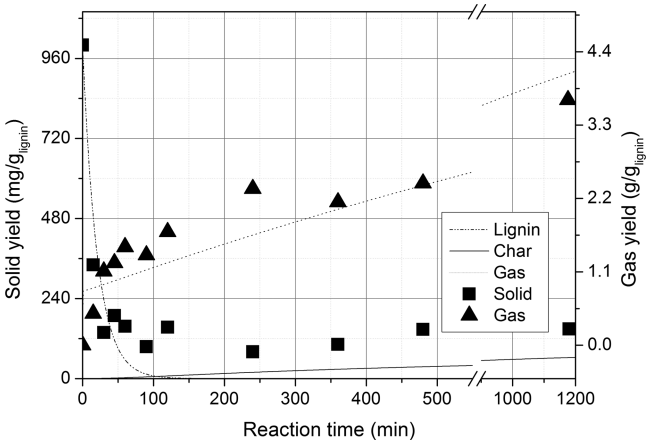

Figure 13. Fits of the gas-lump and the solid residue compared with the experimental data. The differentiation between lignin and char in the solid residue was accomplished largely by FT-IR analysis, as illustrated in Figure 6.

which represent the 3 primary reactions of lignin degradation (k_1, k_6, and k_{10}), one can observe that the reaction to L_D (k_{10}) is the fastest. The fit curve for lignin shows that a total conversion of lignin can be assumed after 100−120 min, which is in good agreement with the results obtained from the FT-IR analysis of the solid residue.

The rate coefficient (Table 3) of the reaction of catechol to phenol (k_4) is very low compared to other coefficients within the model and therefore of minor importance. The same is true for the gasification of phenols (k_5). Ethylation of phenols is the only

Table 3. Rate Coefficients (min^{-1}) of the 17 Defined Reactions within the Developed Model (see Figure 11)

rate coefficient	value (min^{-1})
k_1	7.94×10^{-4}
k_2	8.65×10^{-3}
k_3	1.09×10^{-2}
k_4	2.24×10^{-6}
k_5	5.81×10^{-15}
k_6	3.61×10^{-4}
k_7	1.79×10^{-2}
k_8	1.92×10^{-3}
k_9	5.71×10^{-3}
k_{10}	4.68×10^{-2}
k_{11}	8.32×10^{-4}
k_{12}	4.99×10^{-4}
k_{13}	3.56×10^{26}
k_{14}	2.04×10^{-2}
k_{15}	3.56×10^{-5}
k_{16}	4.16×10^{-5}
k_{17}	1.17×10^{-3}

reaction pathway which is assumed to be reversible. The rate coefficients of ethylation and deethylation are of the same order of magnitude. The ethyl substitution in the *para*- position (k_{14}) is slightly faster than deethylation (k_7), whereas the ethylation in ortho-position (k_8) is about three times slower than deethylation (k_9). Char formation from L_D (k_{16}) is of minor importance compared to the gasification of L_D (k_{11}). Char formation from catechol (k_3) on the other hand is faster than from phenol (k_{17}) or from L_D.

Within the model, polyaromatic components derived from the biomass (L_D) are assumed to decompose directly into gaseous components (k_{11}), but can also form methoxy-phenols (k_{15}) and char (k_{16}). Mathematical fitting showed that the latter route is of minor importance. The fit also confirms that the degradation of formic acid is very fast at given temperatures (k_{13}). The degradation of ethanol (k_{12}) is significantly slower. However, at long reaction times it has to be considered and is of high importance, if a recovery of the solvent ethanol is considered for a technical process.

DISCUSSION

Replicate experiments showed the averaged percentage error for the measured global bulk products solid residue and gas to be 13 and 10 wt %, respectively. Standard deviations for these two average values were calculated to be 6% and 2%, respectively. A possible explanation for this error is found in the determination of the solid residue moisture. Although the solids were weighed before and after drying, it is likely that a certain amount of the volatile moisture attached to the soild residue evaporated during separation of liquids and solids before weighing. Furthermore, the amount of gas was determined volumetrically. The individual gas masses were calculated with the help of standard density of the pure gas components. This leads to a slight overestimation of the weight of the gas.

Gas chromatographic analysis of the liquid product gives results for the yield of 12 different kinds of phenolic components, certainly less than the real number of different phenolic products from lignin depolymerization, but sufficient to evaluate a simple reaction network as suggested by Jegers and Klein for the pyrolysis of lignin.[10] The quality of results is supported by the good fit of the single measurement data points with respect to

dx.doi.org/10.1021/ie301487v | *Ind. Eng. Chem. Res.* 2012, 51, 10595−10606

the calculated yields as shown in Figure 14. The better the fit, the closer the data points plot to the diagonal line.

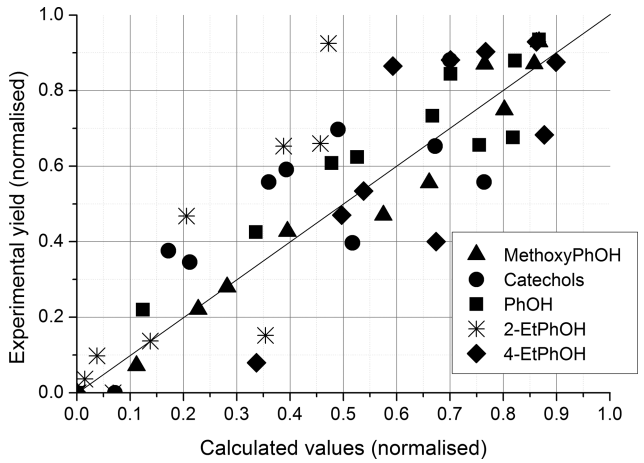

Figure 14. Comparison of calculated and experimental data for product yields of all phenolic (lump) components. Normalizing factors (mg/g_{lignin}): MethoxyPhOH, 14.0, Catechols, 7.0, PhOH, 3.0, 4-EtPhOH, 5.0, 2-EtPhOH, 1.5.

Results from the FT-IR analysis of the solid residue as well as results from the fit of the rate coefficients show that approximately 100 min after starting the reaction, most of the lignin structure has disappeared. Solvolytic cleavage of the ether bonds present in the lignin structure, as already postulated for lignin degradation in a mixture solvent of ethanol and water by Yuan et al., is assumed to be the preferred reaction mechanism.[38]

The observed effects of water on guaiacol pyrolysis describes a further parallel pathway based on the solvation of the guaiacol molecules, thus preventing these from participating in free-radical reactions in order to form high molecular weight material.[35] This reaction pathway is believed to be transferable also to other protic solvent systems as well as lignin. Furthermore, external hydrogen donor sources have been reported to cap the radical moieties with hydrogen, thus reducing the radical concentration, which can be advantageous and suppress repolymerization reactions.[9] The reaction coefficient of the degradation of guaiacol (k_2) under pyrolytic conditions (ca. 0.0084 min^{-1}) obtained by Vuori,[39] is comparable to the value calculated within the fit of this model (0.0087 min^{-1}). However, results for the decomposition of guaiacol after catalytic hydrothermal lignin degradation are in the same order of magnitude, although the value is almost double (0.014 min^{-1}).[6] Thus, whether guaiacols decompose via radical or hydrolytic mechanims is difficult to decide when only considering the rate coefficients. The good agreement of one of the calculated rate coefficients with those found in literature for similar reactions shows that the model is not only a mathematical method for the simulation of experimentally determined values, but also sensible in respect to the chemistry of lignin degradation.

4-Ethyl groups are generally the dominant substituents for all species at lower reaction times. The occurrence of 4-ethylphenol as a primary product strongly suggests that ethyl group substituents are both a product of alkylation reactions in *ortho-* and *para-* position[17] and depolymerization. Supported by the Delplot analysis, it can be concluded that 4-ethylphenol is a primary product of lignin degradation. 2-Ethylphenol, however, is a late product and its yield hardly decreases toward very high reaction times. It is thus assumed that 4-ethylphenol is formed directly from the lignin structure whereas 2-ethylphenol is formed by ethylation of phenols.

Hydrogen donor solvents have been seen to influence various biomass degradation processes. The high yields of ethyl substituted guaiacols, and indeed also catechols and phenols at lower reaction times, may be related to the capping of highly reactive vinyl- (to ethyl-) substituted guaiacol intermediates by these donor solvents.[15,40] This could be part of the reason for the high yield of 4-ethyl and 4-vinyl substituents for the different phenolic species, which in the work of Ye et al. comprised a total of 30% of all lignin derived components quantified.[15]

The comparison of polymerization pathways from catechol (k_3) and phenol (k_{17}) shows that catechols are more prone to repolymerize with k_3 being greater than k_{17}. This agrees with the results obtained by McMillen et al.,[37] who found that especially cresols are able to cap the radical induced coupling of hydroxybenzenes under pyrolysis conditions. The low reaction rates for gas formation from phenol (k_5) furthermore supports the suggestion that monohydroxyl phenols are stable, contrary to the reactive methoxy phenols and catechols.[10]

The model fits experimental values well and the derived rate constants match values found in literature. The number and choice of selected lumps, as well as their interaction pathways, are sufficient to describe the degradation of lignin with a focus on the deoxygenation and ethylation reactions in the production of monoaromatics under the given reaction conditions. Alteration of temperature in the range of 643 to 663 K[29] has been reported to show some systematic variations in the product spectrum, which the model should be able to work with. Reasonable variations of the loadings that do not alter critical ratios are also expected to be correctly described. The model is based on the use of ethanol as solvent medium as a source for ethylation reactions. The general degradation pathways shown in this paper are however also found for alternative hydrogen donor systems,[6] and should thus be transferable to these with minor adaptations. The necessity of the introduced single 4-ethylphenol component suggests that adaptations to the model for different types of lignin would be necessary. The evaluation of the influence of temperature, loading ratios, and type of reactor system are documented by Forchheim et al. in a separate paper,[41] therein describing the robustness and further applicability of the model.

■ CONCLUSIONS

It has been shown that a formal kinetic lump model based on quantitative data of key phenolic components and bulk products can be used to describe reactions of lignin degradation in ethanol in the presence of hydrogen produced by formic acid.

The analysis shows that lignin depolymerization in ethanol is carried out quickly and efficiently at high temperature and pressure conditions. The overall formal reaction rate of the formation of primary products from lignin in our experiments is comparable with that of hydrolytic lignin degradation obtained by Zhang et al.[23] Various ethyl-, methyl- and nonsubstituted phenolic units of varying oxygenation degrees are observed. The observed time dependencies suggest consecutive reactions starting from the monomeric syringol and different guaiacols, whose abundances rapidly decrease with reaction time. These react further accompanied with an increase in the degree of demethoxylation and deoxygenation of the different substituted species to yield catechols and thereafter phenols as stable products.

Further main reaction pathways would be highly dependent on the structure of the lignin used. The high abundance of *para-*coumaryl units within the wheat straw lignin used as feed

material, yielding a high amount of 4-ethylphenol as a primary product, suggests a strong biomass dependence for individual products within the scheme.

High yields of monomeric units are opposed by competing charring and gasification pathways. These are slow in comparison to the depolymerization, however in the competing reactions of repolymerizing catechol to char and further deoxygenation to phenols, the more rapid repolymerization is problematic. A short reaction time for deoxygenation would be beneficial, as the charring vulnerability is lower for deoxygenated phenols than for catechols. It is thus indicated that it will be necessary to catalyze these reaction steps to increase the recovery of demethoxylated phenolics in the produced bio-oil.

■ ASSOCIATED CONTENT

Supporting Information

Additional text, figure, and table. This material is available free of charge via the Internet at http://pubs.acs.org.

■ AUTHOR INFORMATION

Corresponding Author

*E-mail: ursel.hornung@kit.edu.

Author Contributions

§Contributed equally to this work.

Notes

The authors declare no competing financial interest.

■ ACKNOWLEDGMENTS

We thank Statoil's VISTA scholarship program, administered by the Norwegian Academy of Science & Letters and LtL NOR AS for funding of this work. Furthermore, ALM India Pvt. Ltd. is thankfully acknowledged for providing the biomass and communication of sample information to us. We thank Robert Grandl for Matlab support and Birgit Rolli for GC analysis and maintenance.

■ REFERENCES

(1) *Annual Book of ASTM Standards*; ASTM: Philadelphia, PA, 1987; Vol. *05.01*, pp 835−844, ASTMD, 1655−82.

(2) Zhao, W.; Xu, W.-J.; Lu, X.-J.; Sheng, C.; Zhong, S.-T.; Tang, S.-R.; Zong, Z.-M.; Wei, X.-Y. Preparation and property measurement of liquid fuel from supercritical ethanolysis of wheat stalk. *Energy Fuels* **2010**, *24*, 136−144.

(3) Kleinert, M.; Barth, T. Towards a lignincellulosic biorefinery: direct one-step conversion of lignin to hydrogen-enriched biofuel. *Energy Fuels* **2008**, *22*, 1371−1379.

(4) Gellerstedt, G.; Li, J.; Eide, I.; Kleinert, M.; Barth, T. Chemical structures present in biofuel obtained from lignin. *Energy Fuels* **2008**, *22*, 4240−4244.

(5) Mohan, D. Pyrolysis of wood/biomass for bio-oil: a critical review. *Energy Fuels* **2006**, *20*, 848−889.

(6) Forchheim, D.; Hornung, U.; Kruse, A.; Kempe, P.; Steinbach, D. Influence of RANEY nickel on the formation of intermediates in the degradation of lignin. *Int. J. Chem. Eng.* **2012**, DOI: 10.1155/2012/589749.

(7) Pearl, I. W. *The Chemistry of Lignin*; Marcel Dekker Inc., New York, 1967; p 339.

(8) Freudenberg, K.; Neish, A. C. *Constitution and Biosynthesis of Lignin*; Springer Verlag: New York, 1968.

(9) Dorrestijn, E.; Kranenburg, M.; Poinsot, D.; Mulder, P. Lignin depolymerization in hydrogen-donor solvents. *Holzforschung* **1999**, *53*, 611−616.

(10) Jegers, H. E.; Klein, M. T. Primary and secondary lignin pyrolysis reaction pathways. *Ind. Eng. Chem. Process Des. Dev.* **1985**, *24*, 173−183.

(11) Klein, M. T.; Virk, P. S. Model pathways for gas release from lignites. *Prepr. Pap. - Am. Chem. Soc., Div. Fuel Chem.* **1980**, *25*, 180−190.

(12) Nimmanwudipong, T.; Runnebaum, R. C.; Block, D. E.; Gates, B. C. Catalytic conversion of guaiacol catalyzed by platinum supported on alumina: reaction network including hydrodeoxygenation reactions. *Energy Fuels* **2011**, *25*, 3417−3427.

(13) Nimmanwudipong, T.; Runnebaum, R. C.; Block, D. E.; Gates, B. C. Catalytic reactions of guaiacol: reaction network and evidence of oxygen removal in reactions with hydrogen. *Catal. Lett.* **2011**, *141*, 779−783.

(14) Klein, M. T.; Virk, P. S. Modeling of lignin thermolysis. *Energy Fuels* **2008**, *22*, 2175−2182.

(15) Ye, Y.; Zhang, Y.; Fan, J.; Chang, J. Novel method for production of phenolics by combining lignin extraction with lignin depolymerization in aqueous ethanol. *Ind. Eng. Chem. Res.* **2012**, *51*, 103−110.

(16) Miller, J. E.; Evans, L.; Littlewolf, A.; Trudell, D. E. Batch microreactor studies of lignin and lignin model compound depolymerization by bases in alcohol solvents. *Fuel* **1999**, *78*, 1363−1366.

(17) Holmelid, B.; Kleinert, M.; Barth, T. Reactivity and reaction pathways in thermochemical treatment of selected lignin model compounds under hydrogen rich conditions. *J. Anal. Appl. Pyrolysis* **2012**, DOI: 10.1016/J.JAAP.2012.03.007.

(18) Nunn, T. R.; Howard, J. B.; Longwell, J. P.; Peters, W. A. Product compositions and kinetics in the rapid pyrolysis of milled wood lignin. *Ind. Eng. Chem. Process Des. Dev.* **1985**, *24*, 844−852.

(19) Várhegyi, G.; Antal, M. J.; Jakab, E.; Szabó, P. Kinetic modeling of biomass pyrolysis. *J. Anal. Appl. Pyrolysis* **1997**, *42*, 73−87.

(20) Miller, R. S.; Bellan, J. A generalized biomass pyrolysis model based on superimposed cellulose, hemicellulose and lignin kinetics. *Combust. Sci. Technol.* **1997**, *126*, 97−137.

(21) Prakash, N.; Karunanithi, T. Kinetic modeling in biomass pyrolysis - a review. *J. Appl. Sci. Res.* **2008**, *4*, 1627−1636.

(22) Brebu, M.; Vasile, C. Thermal degradation of lignin - a review. *Cellul. Chem. Technol.* **2010**, *44*, 353−363.

(23) Zhang, B.; Huang, H.-J.; Ramaswamy, S. Reaction kinetics of the hydrothermal treatment of lignin. *Appl. Biochem. Biotechnol.* **2011**, *147*, 119−131.

(24) Wahyudiono,; Sasaki, M.; Goto, M. Thermal decomposition of guaiacol in sub- and super-critical water and its kinetic analysis. *J. Mater. Cycles Waste Manage.* **2011**, *13*, 68−79.

(25) Bhore, N.; Klein, M.; Bischoff, K. The Delplot technique: a new method for reaction pathway analysis. *Ind. Eng. Chem. Res.* **1990**, *29*, 313−316.

(26) Lagarias, J. C.; Reeds, J. A.; Wright, M. H.; Wright, P. E. Convergence properties of the Nelder−Mead simplex method in low dimensions. *SIAM J. Optim.* **1998**, *9*, 112−147.

(27) Gasson, J. R.; Kleinert, M.; Barth, T.; Forchheim, D.; Sahin, E.; Kruse, A.; Eide, I. Lignin solvolysis: Upscaling of the Lignin-to-Liquid conversion process towards technical applicability. In *Proceedings of the 18th European Biomass Conference*; Lyon, 2010; pp 10−13.

(28) Yu, J.; Savage, P. Decomposition of formic acid under hydrothermal conditions. *Ind. Eng. Chem. Res.* **1998**, *37*, 2−10.

(29) Kleinert, M.; Gasson, J. R.; Eide, I.; Hilmen, A.-M.; Barth, T. Developing solvolytic conversion of Lignin-to-Liquid (LtL) fuel components: optimization of quality and process factors. *Cellul. Chem. Technol.* **2011**, *45*, 3−12.

(30) Fengel, D.;Wegener, G. *Wood Chemistry Ultrastructure Reactions*; Verlag Kessel: Remagen-Oberwinter, Germany, 1987; pp 151−154.

(31) Roy, A. K.; Bag, S. C.; Sen, S. K. Studies on the chemical nature of milled wood lignin of jute stick. *Cellul. Chem. Technol.* **1987**, *21*, 343−348.

(32) Hergert, H. L. In *Lignins: Occurrence, Formation, Structure and Reaction*, 1st ed.; Sarkanen, K., Ludwig, C., Eds.; Wiley Interscience, New York, 1971; pp 268−272.

(33) Lau, S.; Ibrahim, R. FT-IR spectroscopic studies on lignin from some tropical woods and rattan. *Pertanika* **1992**, *14*, 75−81.

(34) Pasquali, C. E. L.; Herrera, H. Pyrolysis of lignin and IR analysis of residues. *Thermochim. Acta* **1997**, *293*, 39−46.

(35) Lawson, J. R.; Klein, M. T. Influence of water on guaiacol pyrolysis. *Ind. Eng. Chem. Fundam.* **1985**, *24*, 203−208.
(36) Klein, M. T.; Hou, Z.; Bennett, C. Reaction network elucidation: interpreting Delplots for mixed generation products. *Energy Fuels* **2012**, *26*, 52−54.
(37) McMillen, D. F.; Malhotra, R.; Chang, S.-J.; Nigenda, S. E.; John, G. S. Fundamental mechanisms of biomass, pyrolysis and oxidation. *Fuel* **1997**, *83*, 1455−1467.
(38) Yuan, Z.; Cheng, S.; Leitch, M.; Xu, C. Hydrolytic degradation of alkaline lignin in hotcompressed water and ethanol. *Bioresour. Technol.* **2010**, *101*, 9308−9313.
(39) Vuori, A. Pyrolysis studies of some simple coal related aromatic methyl esters. *Fuel* **1986**, *65*, 1575−1583.
(40) Petrocelli, F. P.; Klein, M. T. Model reaction pathways in Kraft lignin pyrolysis. *Macromolecules* **1984**, *17*, 161−169.
(41) Forchheim, D.; Gasson, J. R.; Barth, T.; Hornung, U.; Kruse, A. Modeling the lignin degradation kinetics in a ethanol/formic acid solvolysis approach - Part II: Validation and transfer to variable conditions. *Ind. Eng. Chem. Res.* **2012**, No. 10.1021/ie301489w.